JOURNAL OF MAGNETIC RESONANCE **127,** 217–224 (1997)
ARTICLE NO. MN971197

Multiple Nonlinear Stimulated Echoes

I. Ardelean,*,† R. Kimmich,* S. Stapf,* and D. E. Demco†

*Sektion Kernresonanzspektroskopie, Universität Ulm, 89069 Ulm, Germany; and
†Department of Physics, Technical University, 3400 Cluj-Napoca, Romania

Received January 30, 1997; revised May 17, 1997

Three-pulse sequences in the presence of magnetic field gradients at high magnetic fields produce multiple nonlinear stimulated echoes (NOSE) at times $n\tau_1$ after the third pulse, where n is an integer and τ_1 the interval between the first two pulses. These phenomena are due to the demagnetizing field produced by the spatial modulation of the nuclear magnetization arising in the sample after the first two pulses. The theory is presented and compared with experiments. The dependence of the NOSE amplitudes on the flip angles and on the pulse intervals is described. Implications for multidimensional NMR experiments based on sequences of three or more pulses in the presence of field gradients are discussed.

INTRODUCTION

It is known that NMR experiments based on two or more radiofrequency (RF) pulses can lead to a spatial modulation of the magnetization in certain intervals provided that the magnetic field is inhomogeneous. This in turn modulates the demagnetizing field within the sample so that nonlinear effects arise (*1–9*). Phenomena of this sort have been ignored for a long time because the demagnetizing field is so small compared with the external magnetic field $\mathbf{B}_0$. However, the high fields which are now standard in NMR lead to significant effects on this basis which can no longer be neglected. In particular, the spatially modulated demagnetizing field strongly influences the coherence evolution during a pulse sequence.

In the case of two-pulse experiments carried out in a strong magnetic field while a magnetic field gradient is present, *multiple spin echoes* (MSE) appear in addition to the conventional Hahn echo (*1–9*). Furthermore, apart from the ordinary *stimulated echo* (STE), *multiple nonlinear stimulated echoes* (NOSE) were predicted and observed after the RF pulse sequence (*10*)

$$(\pi/2)_X - \tau_1 - (\pi/2)_Y - \tau_2 - (\alpha)_Y,$$

in the presence of a field gradient. The ordinary stimulated echo arises at time τ_1 after the third pulse, whereas the multiple nonlinear stimulated echoes are generated at times $2\tau_1$ (NOSE1), $3\tau_1$ (NOSE2), and so on. The echo amplitude decreases with increasing NOSE order. In addition, we have also observed multiple echoes at times $\tau = n\tau_1 + m\tau_2$ after the third RF pulse (where n and m are integers) in cases when the transverse magnetization was not completely spoiled at the end of the τ_2 interval. The condition is that the magnetic field is large enough and possesses a periodic inhomogeneity.

The origin of all these phenomena is the demagnetizing field $B_d(\mathbf{r})$ discussed in Refs. (*1–6*). The expression of the demagnetizing field, which generally is a complicated function of the shape of the sample, can easily be evaluated if a constant field gradient G of sufficient strength is applied along the $\hat{\mathbf{s}}$ direction in the sample (*5*).

Immediately after the first RF pulse the magnetization is uniform in the sample. It then develops into a spatial helix along the $\hat{\mathbf{s}}$ direction with a pitch $p = 2\pi/(\gamma G t)$ determined by the field gradient and the evolution time. The demagnetizing field is small enough so that the helix formation due to the field gradient is not disturbed. Since the proportionality $B_\mathrm{d} \sim \mu_0 M_0$ applies, the demagnetizing field is negligible compared with the magnetic field variation in the sample of length l (*5*), i.e.,

$$\mu_0 M_0 \frac{1}{Gl} \ll 1. \qquad [1]$$

If this condition is fulfilled for times $t > 2\pi/(\gamma G l)$, the helical magnetization over the sample produces a simple helical demagnetizing field $\mathbf{B}_\mathrm{d}(s)$ (*5*). This demagnetizing field produces only a small modulation of the precession frequency because the component of $\mathbf{B}_\mathrm{d}(s)$ parallel to $\mathbf{M}(s)$ does not affect the evolution of the magnetization.

The demagnetizing field is expected to have a relevant contribution at times for which the magnetic field variation over the helix pitch $(2\pi/\gamma G t)G$ is smaller than $B_\mathrm{d} \sim \mu_0 M_0$, i.e., with the condition (*5*)

$$\gamma \mu_0 M_0 t > 1 \qquad [2]$$

1090-7807/97 $25.00

and $t \ll T_2$. Furthermore, the pitch of the spatial helix must be large enough so that self-diffusion does not become effective (*5*); that is,

$$D(\gamma G)^2 t^3 \ll 1. \quad [3]$$

We note that conditions [1] and [2] are independent of each other. The demagnetizing field has a significant effect if condition [2] is fulfilled even if condition [1] is not. However, in this case the mathematical treatment of the problem is not so simple. On the other hand, conditions [1] and [3] are interdependent, but can be met simultaneously. Also, condition [2] is not critical for obtaining an observable effect of the demagnetizing field. It is rather sufficient that $\gamma\mu_0 M_0 t$ should not be much smaller than one.

The evolution of the magnetization during the pulse sequence $(\alpha_1)_X - \tau - (\alpha_2)_X$ has been studied by several authors using modified Bloch equations (*5, 7–9, 11, 12*). However, an exact solution of Bloch equations is sometimes difficult to obtain because of the nonlinear character of these equations owing to the influence of the demagnetizing field. A quantum mechanical approach was introduced in Refs. (*2, 4*) (and references therein). A semiclassical procedure, which will be used in the present work, was discussed more recently in Ref. (*1*), employing the spin operator formalism. In our present work, we will use the same procedure as in Ref. (*1*), where relaxation is taken into account empirically in analogy with the Bloch equations used in Ref. (*13*) to characterize an inhomogeneous mixed echo. This method avoids solving complicated coupled differential equations and its results are not restricted by the condition $\gamma\mu_0 M_0 \tau_1 < 1$ which reduces the effect of the demagnetizing field. In this case the echoes due to higher-order harmonics can also be easily computed. The semiclassical formalism discussed below is more elegant in the evaluation of NMR observables and the effect of the radiofrequency pulses. Nevertheless, direct solution of the Bloch equations can also be used to predict the existence of nonlinear multiple echoes.

In order to keep the theory as compact as possible we will restrict ourselves in the following to the pulse sequence $(\pi/2)_X - \tau_1 - (\pi/2)_Y - \tau_2 - (\alpha)_Y$. Note that the choice of the pulse phases is not critical for the formation of multiple nonlinear stimulated echoes. Our theoretical results were probed using a sample of poly(dimethylsiloxane) which allowed us to neglect signal attenuation due to self-diffusion.

THEORY

In the following we consider an ensemble of isolated spins $I = \frac{1}{2}$ in a static magnetic field $\mathbf{B}_0$ and a constant field gradient G along the z direction. The equilibrium density operator at position z in the sample in the high-temperature approximation is given by

$$\rho(0^-) = a + bI_z, \quad [4]$$

where $a = 1/\mathrm{Tr}\{E\}$, $b = \gamma\hbar B_0/(k_B T\ \mathrm{Tr}\{E\})$, and $I_z = \Sigma_i I_{iz}$, with $i = 1, \ldots, N$. N represents the number of spins in the volume element at the z position in the sample. Here $\mathrm{Tr}\{E\} = N(2I+1)^N$ describes the trace of the unity operator for a system of N spins in a volume element. Because the constant a in the density operator representation is not affected by evolution operators it will be disregarded in the following.

Immediately before the application of the first pulse the magnetization in the sample is given by

$$M_0 = \gamma\hbar N\ \mathrm{Tr}\{\rho(0^-) I_z\}. \quad [5]$$

As we are interested in the magnetization evolution, we can consider in the following a reduced spin density operator

$$\sigma(0^-) = I_z, \quad [6]$$

where σ is the reduced density operator defined by omitting all constant terms and factors implied in ρ.

In the course of the pulse sequence the spin coherences evolve under the action of ''hard'' pulses (i.e., the pulse amplitude B_1 is assumed to be much larger than the field offset Gz) and the rotating-frame Hamiltonian (*1, 2*)

$$H(z, t) = -\gamma\hbar[Gz + \mu_0 M_z(z, t)] I_z. \quad [7]$$

Here the second term represents the contribution of the demagnetizing field at position z (*1, 2*).

In general the evolution between two pulses during a time τ under the action of the rotating-frame Hamiltonian Eq. [7] is described by the nonlinear equation for the reduced density operator,

$$i\hbar \frac{\partial\sigma(z, t)}{\partial t} = [H(z, t), \sigma(z, t)], \quad [8]$$

which is not to be identified with the Liouville/von Neumann equation (*2*) because of the nonlinear character. The formal solution of the above equation corresponds (*1*) to a rotation of the I_x and I_y components of the spin operator around the z axis by an angle

$$\varphi(z, \tau) = \int_0^\tau \gamma[Gz + \mu_0 M_z(z, t)]\, dt. \quad [9]$$

This rotation affects only the I_x and I_y components of the I-spin operator.

Relaxation effects can be taken into account in a phenomenological way (*13*) according to the solutions of the conven-

tional Bloch equations. The evolution of the reduced spin density operator can first be treated independently of relaxation, generally resulting in

$$\sigma(z, t) = c_x(z, t)I_x + c_y(z, t)I_y + c_z(z, t)I_z. \quad [10]$$

In a second step, the coefficients c_x, c_y, c_z in the reduced density operator are replaced by new coefficients c_x', c_y', c_z' now implying relaxational attenuation according to

$$\begin{aligned} c_x' &= c_x e^{-t/T_2}, \\ c_y' &= c_y e^{-t/T_2}, \\ c_z' &= (c_z - 1)e^{-t/T_1} + 1. \end{aligned} \quad [11]$$

In the present computation we assume $\tau_1 \leqslant T_2$ and $T_2 < \tau_2 < T_1$. The latter condition means that the spin coherences at the end of the second interval can be neglected and, hence, any echoes produced by the third pulse on this basis.

Just after the action of the first RF pulse, $(\pi/2)_X$ at time $t = 0^+$, the reduced density operator is

$$\sigma(0^+) = I_y. \quad [12]$$

The evolution between the first and the second RF pulses is governed by the Hamiltonian [7]. The reduced density operator takes the form

$$\sigma(z, \tau_1^-) = I_y \cos\varphi(z, \tau_1) + I_x \sin\varphi(z, \tau_1) \quad [13]$$

in the absence of relaxation, and

$$\begin{aligned} \sigma'(z, \tau_1^-) = {} & I_y e^{-\tau_1/T_2} \cos\varphi(z, \tau_1) \\ & + I_x e^{-\tau_1/T_2} \sin\varphi(z, \tau_1) \end{aligned} \quad [14]$$

with relaxation taken into account. As can be seen from Eq. [14], the local transverse magnetization develops into a spatial helix after the first pulse. The helix pitch is $p = 2\pi/(\gamma G \tau_1)$ and decreases with increasing evolution time. Note that, by contrast, the z component of the magnetization is still uniformly distributed in the sample so that no demagnetizing-field effect arises yet. That is, $\varphi(z, \tau_1) = \gamma G z \tau_1$.

The second pulse $(\pi/2)_Y$ affects only the I_x and I_z components of the I-spin operator so that

$$\begin{aligned} \sigma'(z, \tau_1^+) = {} & I_y e^{-\tau_1/T_2} \cos\varphi(z, \tau_1) \\ & + I_z e^{-\tau_1/T_2} \sin\varphi(z, \tau_1). \end{aligned} \quad [15]$$

Beginning with this moment the evolution of the reduced density operator is influenced by the demagnetizing field produced by the M_z component of the local magnetization.

The rotating-frame Hamiltonian acts only on the I_x and I_y components of the I-spin operator during this time interval. Assuming complete relaxation of all coherences in the τ_2 interval, the reduced density operator just before the third pulse ($t = \tau_1 + \tau_2^-$) becomes

$$\begin{aligned} \sigma'(z, \tau_1 + \tau_2^-) = I_z [& e^{-\tau_1/T_2} e^{-\tau_2/T_1} \sin\varphi(z, \tau_1) \\ & - e^{-\tau_2/T_1} + 1]. \end{aligned} \quad [16]$$

The third pulse $(\alpha)_Y$ rotates the I_z component of the I-spin operator and leads to

$$\begin{aligned} \sigma'(z, \tau_1 + \tau_2^+) = {} & I_z [e^{-\tau_1/T_2} e^{-\tau_2/T_1} \sin\varphi(z, \tau_1) \\ & - e^{-\tau_2/T_1} + 1] \cos\alpha \\ & - I_x [e^{-\tau_1/T_2} e^{-\tau_2/T_1} \sin\varphi(z, \tau_1) \\ & - e^{-\tau_2/T_1} + 1] \sin\alpha. \end{aligned} \quad [17]$$

As can readily be seen, the magnetization is split into two components modulated along the z direction. The transverse component evolves in the presence of the demagnetizing field created by the longitudinal component. Since the longitudinal component is not changed by free evolution, and because it will not contribute to the signal, we focus on the transverse magnetization components. The corresponding reduced density operator just after the third RF pulse is

$$\begin{aligned} \sigma'(z, \tau_1 + \tau_2^+) = -I_x [& e^{-\tau_1/T_2} e^{-\tau_2/T_1} \sin\varphi(z, \tau_1) \\ & - e^{-\tau_2/T_1} + 1] \sin\alpha. \end{aligned} \quad [18]$$

The evolution after the third RF pulse can be described as a rotation of the I_x component of the I-spin operator around the z axis by an angle

$$\varphi(z, \tau) = \gamma G z \tau + \xi(\tau) \sin\varphi(z, \tau_1) + \delta(\tau), \quad [19]$$

where

$$\xi(\tau) = \gamma \mu_0 M_0 \tau e^{-\tau_1/T_2} e^{-\tau_2/T_1} \cos\alpha. \quad [20]$$

The quantity

$$\delta(\tau) = \gamma \mu_0 M_0 \tau (1 - e^{-\tau_2/T_1}) \cos\alpha \quad [21]$$

represents a phase shift due to relaxation during the τ_2 interval.

Taking into account transverse relaxation effects we obtain the following expression for the reduced density operator at a time τ after the third pulse:

$$\sigma'(z, \tau_1 + \tau_2 + \tau) = [I_y \sin \varphi(z, \tau) - I_x \cos \varphi(z, \tau)] \times [e^{-\tau_1/T_2} e^{-\tau_2/T_1} \sin \varphi(z, \tau_1) - e^{-\tau_2/T_1} + 1] e^{-\tau/T_2} \sin \alpha. \quad [22]$$

This expression determines the evolution of the complex magnetization after the third pulse,

$$M_+(z, \tau) = M_x + iM_y \propto \mathrm{Tr}\{\sigma'(z, \tau_1 + \tau_2 + \tau)(I_x + iI_y)\}$$

$$M_+(z, \tau) = i \frac{M_0}{2} e^{-(\tau_1+\tau)/T_2} e^{-\tau_2/T_1} \sin \alpha \{e^{i[\varphi(z,\tau_1)-\varphi(z,\tau)]} - e^{-i[\varphi(z,\tau_1)+\varphi(z,\tau)]}\} - M_0(1 - e^{-\tau_2/T_1}) e^{-\tau/T_2} e^{-\varphi(z,\tau)} \sin \alpha, \quad [23]$$

where the phase shift $\delta(\tau)$ has been omitted because it does not affect the amplitude of the echoes. The complex magnetization can be written in a more convenient form using the Bessel function expansion (*4, 5*)

$$e^{i\xi(\tau)\sin\varphi(z,\tau_1)} = \sum_{n=-\infty}^{+\infty} J_n(\xi(\tau)) e^{in\varphi(z,\tau_1)}, \quad [24]$$

and the properties of Bessel functions $J_n(\xi)$ of integer order (*14*)

$$J_{n-1}(\xi) - J_{n+1}(\xi) = 2 \frac{d}{d\xi} [J_n(\xi)] \quad [25]$$

and

$$J_{-n}(\xi) = (-1)^n J_n(\xi). \quad [26]$$

Using the expansion [24], the complex magnetization can be rewritten as

$$M_+(z, \tau) = iM_0 \sin \alpha \, e^{-\tau/T_2} \times \sum_{n=-\infty}^{+\infty} (-1)^{n+1} \{e^{-\tau_2/T_1} e^{-\tau_1/T_2} \frac{\partial}{\partial \xi} [J_n(\xi(\tau))] + i(1 - e^{-\tau_2/T_1}) J_n(\xi(\tau))\} e^{-i\gamma G z (n\tau_1 - \tau)}. \quad [27]$$

For the signal of the entire sample we are interested in an average of $M_+(z, \tau)$ over all positions in the sample. This average will be zero unless it is independent of position. This is fulfilled for those time moments after the third pulse for which $\tau = n\tau_1$. For these time moments multiple nonlinear stimulated echoes will appear. The amplitudes of these echoes are proportional to the average complex magnetization

$$\langle M_+(n\tau_1) \rangle = (-1)^{n+1} iM_0 \times \sin \alpha \{ie^{-(n+1)\tau_1/T_2} e^{-\tau_2/T_1} \times \frac{\partial}{\partial \xi} [J_n(\xi(n\tau_1))] + ie^{-n\tau_1/T_2}(1 - e^{-\tau_2/T_1}) \times J_n(\xi(n\tau_1))\}, \quad [28]$$

which can easily be computed for each of these echoes. Restricting the computation to the first terms of the series expansion of the Bessel functions (*14*) leads to echo amplitudes at times $\tau = n\tau_1$ proportional to

$$\langle M_+(n\tau_1) \rangle \cong (-1)^{n+1} \frac{i}{2^n (n-1)!} M_0 \times \sin \alpha \, e^{-2n\tau_1/T_2} e^{-n\tau_2/T_1} \times (\gamma \mu_0 M_0 \cos \alpha \, n\tau_1)^{n-1} \times [1 + i(\gamma \mu_0 M_0 \cos \alpha \, \tau_1) \times (1 - e^{-\tau_2/T_1})]. \quad [29]$$

In the limit $\gamma \mu_0 M_0 \tau_1 \ll 1$ it is sufficient to consider only the first term of Eq. [29]. The first echo, i.e., the conventional stimulated echo, appearing at $\tau = \tau_1$ after the third pulse ($n = 1$) is then expected to have an amplitude proportional to

$$\langle M_+(\tau_1) \rangle = \frac{i}{2} M_0 e^{-2\tau_1/T_2} e^{-\tau_2/T_1} \sin \alpha. \quad [30]$$

The condition $\gamma \mu_0 M_0 \tau_1 \ll 1$ means that the amplitude of this echo is not perceptibly affected by the demagnetizing field. Otherwise even the conventional stimulated echo is expected to be modified by this sort of phenomena.

The amplitudes of the second and the third echoes, appearing at $\tau = 2\tau_1$ and $\tau = 3\tau_1$, respectively, are also readily obtained from Eq. [29]. In the same approximation we may truncate the Bessel series after the first term. The results are

$$\langle M_+(2\tau_1) \rangle = -\frac{i}{4} M_0^2 \gamma \mu_0 \tau_1 e^{-4\tau_1/T_2} e^{-2\tau_2/T_1} \sin(2\alpha) \quad [31]$$

and

$$\langle M_+(3\tau_1) \rangle = i \frac{9}{32} M_0^3 (\gamma \mu_0 \tau_1)^2 e^{-6\tau_1/T_2} e^{-3\tau_2/T_1} \times \sin(2\alpha) \cos \alpha, \quad [32]$$

respectively.

The appearance of nonlinear stimulated echoes obviously depends on the flip angle α of the third pulse. The maximum of NOSE1 is expected for $\alpha = \pi/4$. That of NOSE2 is reached for a somewhat smaller value. On the other hand, no multiple nonlinear stimulated echoes arise if the flip angle of the third pulse is $\alpha = \pi/2$, i.e., if it is adjusted to the value for which the conventional stimulated echo adopts its maximum amplitude. Perhaps this is why multiple nonlinear stimulated echoes have not been discovered up to now.

In the above treatment we have assumed that the first two RF pulses cause flip angles of $\pi/2$. These are the optimal values for the stimulated echo generation. However, nonlinear stimulated echoes of correspondingly reduced amplitudes will also appear for other flip angles as long as an angle of π is avoided.

EXPERIMENTAL

The experiments were carried out on a Bruker MSL 300 spectrometer ($B_0 \approx 7$ T) using 5-mm sample tubes filled to a height of 25 mm. As a test substance we have chosen linear poly(dimethylsiloxane) (PDMS, purchased from Polysciences, Warrington, PA). The weight-averaged molecular weight is $M_W = 17{,}000$, and the room-temperature relaxation times are roughly $T_1 \approx 1.3$ s and $T_2 \approx 0.3$ s. At the temperature of the experiments (293 K), the average self-diffusion coefficient of this polydisperse PDMS sample was measured as 2.3×10^{-12} m^2/s. The equilibrium magnetization M_0 in the field of $B_0 = 7.05$ T was computed to be 0.016 A/m. A constant gradient of $G = 0.7$ mT/m was applied along the z direction. In the complete ranges of the pulse spacings τ_1 and τ_2 used in our investigations, condition [3] was met so that the influence of self-diffusion was negligible. Furthermore, $\mu_0 M_0/Gl \approx 10^{-3}$ which justifies, according to Eq. [1], the above treatment of the influence of the demagnetizing field.

The RF pulse width for a flip angle $\pi/2$ was 18 μs. Proper choice of the pulse delays avoided superpositions with the linear echoes occurring at $\tau_2 - \tau_1$, τ_2, and $\tau_2 + \tau_1$ after the third pulse, respectively (*1*), as well as refocusing of multiple spin echoes (*5, 7–9*) after the third RF pulse. In our experiment a suitable pulse phase and receiver phase cycle was chosen in order to avoid the overlap of the conventional stimulated echo and multiple nonlinear stimulated echoes. The appearance of multiple nonlinear stimulated echoes is not restricted to certain pulse phases.

Higher-order multiple nonlinear echoes at $n\tau_1 + m\tau_2$ after the third pulse were observed up to $m = 2$ and $n = 3$. The fact that some of these echoes possessed intensities comparable to the intensity of the first nonlinear stimulated echo (NOSE1) at $\tau = 2\tau_1$ permitted their identification and the determination of their dependences on pulse lengths and pulse delays.

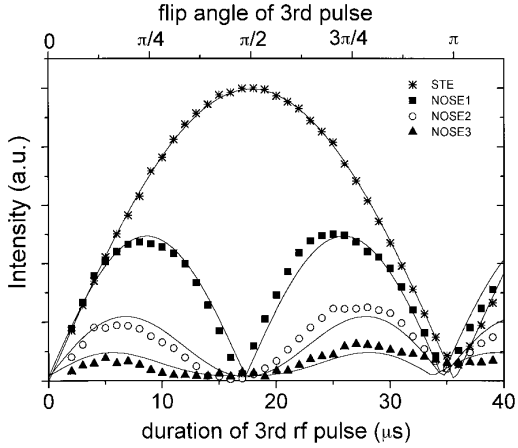

FIG. 1. Intensity of the stimulated echo (STE) at $\tau = \tau_1$ and of the nonlinear multiple stimulated echoes at $\tau = 2\tau_1$ (NOSE1), at $\tau = 3\tau_1$ (NOSE2), and at $\tau = 4\tau_1$ (NOSE3) as a function of the flip angle of the third RF pulse. The times refer to the delay after the third RF pulse. The width of the third RF pulse was varied between 2 and 39 μs. The duration of the RF pulse corresponding to a flip angle of $\pi/2$ was independently determined to be 18 μs. In the pulse sequence $(\pi/2)_X - \tau_1 - (\pi/2)_Y - \tau_2 - (\alpha)_Y$, the delays were set to $\tau_1 = 70$ ms and $\tau_2 = 450$ ms. A total of 16 (stimulated echo) and 280 transients (nonlinear stimulated echoes) with a repetition time of 8 s were accumulated. As a sample, poly(dimethylsiloxane) (PDMS) with a weight-averaged molecular weight of $M_W = 17{,}000$ at $T = 293$ K was used. The solid lines represent best fits of Eqs. [30]–[32]. The echo intensities are not plotted to scale.

RESULTS

The echoes appearing at $\tau = \tau_1, 2\tau_1, 3\tau_1, 4\tau_1$ after the third RF pulse were investigated with respect to the dependence of the echo amplitude on the flip angle of the third pulse. The pulse spacings were chosen to be $\tau_1 = 70$ ms and $\tau_2 = 450$ ms. Figure 1 represents the dependence of the magnitude of four echoes on the length of the third RF pulse. The conventional stimulated echo appearing at $\tau = \tau_1$ is found to possess a maximum intensity for a pulse length of 18 μs corresponding to a flip angle $\pi/2$, as expected. Note that the maximum echo intensity is generally shifted toward smaller flip angles when n increases. This feature becomes quite obvious in Fig. 1. The solid lines represent best fits of Eqs. [30]–[32]. The theoretical curves describe the experimental data very well. Minor deviations are due to imperfections of the pulse length caused by RF field inhomogeneities or by overlapping signals from preceding echoes.

The dependence on the separation between the second and third RF pulses, τ_2, was investigated for $\alpha = \pi/4$. The results are shown in Fig. 2 for $\tau_1 = 50$ ms. From Eqs. [30]–[32], one expects a faster decay for higher-order echoes, corresponding to a time constant of T_1/n for the echoes occurring at $n\tau_1$ after the third pulse. A best fit of Eqs. [30]–[32] results in an average longitudinal relaxation time

of 1260 ± 30 ms. The value obtained by inversion-recovery measurements under identical conditions is 1320 ms (*15*). Although the correct Bessel function representation has been used for the fitting procedure, a deviation from an exponential signal decay is not observable. The coincidence of the T_1 values measured with the different experimental schemes is remarkably good. This shows that the effect of spin–lattice relaxation on the demagnetizing field was negligible as anticipated in our treatment.

The amplitudes of the nonlinear stimulated echoes are expected to first increase proportional to τ_1 until transverse relaxation losses become dominant. Performing the first derivative of Eqs. [30]–[32], with respect to τ_1, renders the maximum intensities of the echoes:

$$\frac{d}{d\tau_1}\langle M_+(n\tau_1)\rangle = 0 \Leftrightarrow \tau_1^{\max} = \frac{n-1}{2n}T_2. \qquad [33]$$

The experimental results for a constant τ_2 of 750 ms are presented in Fig. 3 (intensities not to scale). Solid lines represent best fits according to Eqs. [30]–[32]. With the above-mentioned restrictions, a general agreement with the theoretical predictions is achieved. In particular, the maxima of the NOSE1 and NOSE2 are found near $\tau_1 = T_2/4$ and $\tau_1 = T_2/3$, respectively, where $T_2 = 260$ ms was evaluated from the decay of the stimulated echo. Note that under the conditions chosen for our experiment, the molecular weight

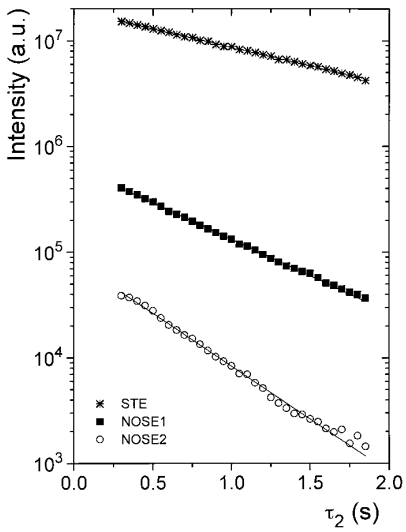

FIG. 2. Intensity of the stimulated echo (STE) at $\tau = \tau_1$ and the nonlinear multiple stimulated echoes at $\tau = 2\tau_1$ (NOSE1) and at $\tau = 3\tau_1$ (NOSE2) after the third RF pulse, respectively, for PDMS 17,000 at $T =$ 293 K as a function of τ_2; τ_1 was set to 50 ms, $\alpha = \pi/4$. A total of 16 (stimulated echo) and 280 transients (nonlinear echoes) with a repetition time of 8 s were accumulated. The solid lines represent best fits of Eqs. [30]–[32]. The echo intensities are plotted to scale.

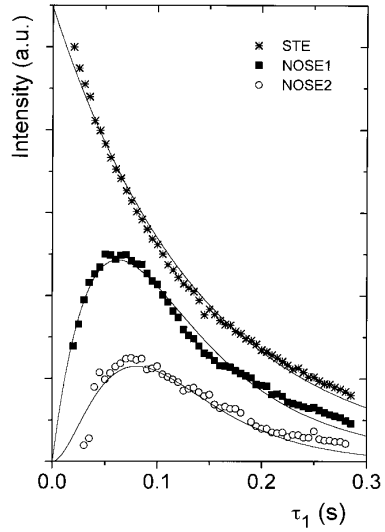

FIG. 3. Intensity of the stimulated echo (STE) at $\tau = \tau_1$ and the multiple nonlinear stimulated echoes at $\tau = 2\tau_1$ (NOSE1) and at $\tau = 3\tau_1$ (NOSE2) after the third RF pulse, respectively, for PDMS 17,000 at $T =$ 293 K as a function of τ_1; τ_2 was set 750 ms, $\alpha = \pi/4$. A total of 40 (stimulated echo) and 320 transients (nonlinear echoes) with a repetition time of 8 s were accumulated. The solid lines represent best fits of Eqs. [30]–[32]. The echo intensities are not plotted to scale.

of the PDMS sample is still below the critical mass ($M_c \approx$ 20,000). That is, transverse relaxation is monoexponential as it was observed before (*15*). The experimental results can be well described by the time dependences given in Eqs. [30]–[32], and thus justify the assumptions made in our treatment. In addition, a comparison of the relative echo intensities may provide a direct measure of the strength of the demagnetizing field.

The existence of high-order multiple nonlinear echoes at $n\tau_1 + m\tau_2$ after the third pulse is shown in Fig. 4. The acquisition started just before the first RF pulse. The ordinary spin echoes following the last pulse appear at τ_1(a), τ_2(f), $\tau_2 - \tau_1$(e), and $\tau_1 + \tau_2$(g). The nonlinear spin echoes appearing at time moments $2\tau_1$(b), $4\tau_1$(c), $\tau_2 - 2\tau_1$(d), $\tau_2 + 2\tau_1$(h), $2\tau_2 - 2\tau_1$(i), $2\tau_2$(j), and $2\tau_1 + 2\tau_2$(k) are also evidenced. The amplitudes of the stimulated echo appearing at τ_1(a) and of the nonlinear stimulated echo at $3\tau_1$ are canceled, as well as the amplitudes of the other conventional echoes appearing at $\tau_2 - \tau_1$(e) and $\tau_2 + \tau_1$(g) because of the phase cycle used. Residual signals at these positions are due to imperfections in the pulse length at different positions in the sample. This pulse phase cycle was chosen so that the stimulated echo did not overlap the nonlinear stimulated signal.

DISCUSSION

Multiple nonlinear stimulated echoes were treated using a semiclassical formalism in which the effects of RF pulses

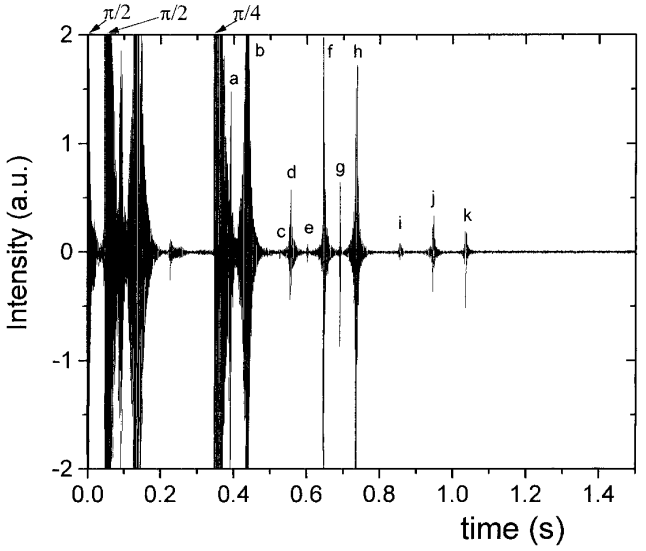

FIG. 4. Echo trains following the third pulse of the sequence $(\pi/2)_X-\tau_1-(\pi/2)_Y-\tau_2-(\pi/4)_Y$. The pulse intervals were $\tau_1 = 45$ ms and $\tau_2 = 300$ ms. The $\pi/2$ pulses were set to 18 μs and $\pi/4$ to 9 μs. A total of 1000 transients with repetition time of 8 s were accumulated. The letters a, b, . . . , k indicate the echoes as explained in the text. As a sample PDMS 17,000 at $T = 293$ K was used.

were evaluated by quantum mechanical formalism and the effect of the demagnetizing field was treated clasically. This is appropriate in view of the semiclassical nature of the phenomena: Free evolution of the coherences does not change the z component of the magnetization which is responsible for the demagnetizing-field effects. That is, apart from relaxation, the spin Hamiltonian is stationary in the free-evolution periods.

The dependences of the echo amplitude on the flip angles and pulse delays were verified in a series of experiments carried out with PDMS. In this way hitherto unknown demagnetizing-field phenomena became obvious. Note that the coherence pathway leading to NOSE signals implies longitudinal magnetization in the τ_2 interval. That is, the observed echoes are *stimulated echoes* by definition. Potential contributions by multiple-quantum coherence or dipolar-order transfer echoes which can arise in principle due to residual long-range intermolecular dipolar couplings can be neglected because of the long τ_2 intervals. This is corroborated by the peculiar dependences on the flip angle of the third pulse which reveals maxima for odd multiples of $\pi/4$ while the flip angles of the first two pulses are kept at $\pi/2$ (Fig. 1).

The NOSE signals may be important for all experiments based on sequences of three or more RF pulses applied in combination with field gradients at high magnetic fields (*2–4, 16*). It is already known that multiple spin echoes affect two-dimensional NMR spectroscopy (*6, 16–19*) utilizing pulsed magnetic field gradients. ''Spurious'' cross peaks arising on this basis might even lead to misinterpretations.

On the other hand, the demagnetizing-field effects may also serve as a source of information. Recently a method for the extraction of structural information using the demagnetizing field has been proposed in Ref. (*19*). This can be done because in the presence of a spatially modulated magnetization the demagnetizing field experienced by a particular spin results predominantly from the magnetization within a region extended less than the spatial period of modulation. Thus, the structure can be probed on different length scales by varying this period of spatial modulation. A Fourier-space relationship between the structure of heterogeneous samples and the amplitude of multiple spin echoes was established on this basis (*20, 21*). NOSE experiments of an analogous type might be of interest.

A demagnetizing-field method was considered for multicomponent liquids where one of the spin species is indirectly detected via the NMR signal of the second spin species (*11*). This method neither requires that the spins of the two species be directly chemically bound nor requires that they be located in the same molecule. Rather it is based on the fact that the spins of the first species precess under the influence of the demagnetizing field produced by the second sort of spins. Effects of this sort should be reconsidered in the light of our NOSE experiments.

Another possible application of the demagnetizing field has been suggested in Ref. (*11*) for diffusion measurements using a single gradient pulse. It is clear that NOSE signals are predestinated for diffusometry as stimulated echoes are in conventional measuring schemes.

ACKNOWLEDGMENT

One of the authors (I.A.) is indebted to the Deutscher Akademischer Austauschdienst (DAAD) for a research fellowship.

REFERENCES

1. R. Kimmich, ''NMR: Tomography, Diffusometry, Relaxometry,'' Springer-Verlag, Berlin, 1997.
2. J. Jeener, A. Vlassenbroek, and P. Broekaert, *J. Chem. Phys.* **103,** 1309 (1995).
3. A. Vlassenbroek, J. Jeener, and P. Broekaert, *J. Magn. Reson. A* **118,** 234 (1996).
4. S. Lee, W. Richter, S. Vathyam, and W. S. Warren, *J. Chem. Phys.* **105,** 874 (1996).
5. G. Deville, M. Bernier, and J. M. Delrieux, *Phys. Rev. B* **19,** 5666 (1979).
6. M. H. Levitt, *Concepts Magn. Reson.* **8,** 77 (1996).
7. W. Dürr, D. Hentschel, R. Ladebek, R. Oppelt, and A. Oppelt, Abstracts of the Society of Magnetic Resonance in Medicine, 8th Annual Meeting, p. 1173, 1989.
8. R. Bowtell, R. M. Bowley, and P. Glover, *J. Magn. Reson.* **88,** 643 (1990).

9. D. Einzel, G. Eska, Y. Hirayoshi, T. Kopp, and P. Wölfle, *Phys. Rev. Lett.* **53,** 2312 (1984).

10. I. Ardelean, S. Stapf, D. E. Demco, and R. Kimmich, *J. Magn. Reson.* **124,** 506 (1997).

11. R. Bowtell, *J. Magn. Reson.* **100,** 1 (1992).

12. P. Robyr and R. Bowtell, *J. Magn. Reson. A* **121,** 206 (1996).

13. D. E. Demco, A. Johansson, and J. Tegenfeldt, *J. Magn. Reson. A* **110,** 183 (1994).

14. P. M. Morse and H. Feshbach, ''Methods of Theoretical Physics,'' McGraw–Hill, New York, 1953.

15. R. Kimmich, M. Köpf, and P. Callaghan, *J. Polym. Sci.: Polym. Phys. Ed.* **29,** 1025 (1991).

16. D. L. Mattielo, W. S. Warren, L. Mueller, and B. T. Farmer II, *J. Am. Chem. Soc.* **118,** 3253 (1996).

17. Q. He, W. Richter, S. Vathyam, and W. S. Warren, *J. Chem. Phys.* **98,** 6779 (1993).

18. W. S. Warren, W. Richter, A. S. Andreatti, and B. T. Farmer II, *Science* **262,** 2005 (1993).

19. W. Richter, S. Lee, W. S. Warren, and Q. He, *Science* **267,** 654 (1995).

20. R. Bowtell and P. Robyr, *Phys. Rev. Lett.* **76,** 4971 (1996).

21. P. Robyr and R. Bowtell, *J. Chem. Phys.* **106,** 467 (1997).